



Published in final edited form as:

Pflugers Arch. 2009 May ; 458(1): 77–88. doi:10.1007/s00424-008-0589-z.

Function and Regulation of Claudins in the Thick Ascending Limb of Henle

Dorothee Günzel¹ and Alan S. L. Yu²

¹Department of Clinical Physiology, Charité, Campus Benjamin Franklin, 12200 Berlin, Germany

²Departments of Medicine and Physiology, University of Southern California Keck School of Medicine, Los Angeles, California 90089

SUMMARY

The thick ascending limb of Henle mediates transcellular reabsorption of NaCl while generating a lumen-positive voltage that drives passive paracellular reabsorption of divalent cations. Disturbance of paracellular reabsorption leads to Ca²⁺ and Mg²⁺ wasting in patients with the rare inherited disorder of familial hypercalciuric hypomagnesemia with nephrocalcinosis (FHHNC). Recent work has shown that the claudin family of tight junction proteins form paracellular pores and determine the ion selectivity of paracellular permeability. Importantly, FHHNC has been found to be caused by mutations in two of these genes, claudin-16 and -19, and mice with knockdown of claudin-16 reproduce many of the features of FHHNC. Here, we review the physiology of TAL ion transport, present the current view of the role and mechanism of claudins in determining paracellular permeability, and discuss the possible pathogenic mechanisms responsible for FHHNC.

INTRODUCTION

Tight junctions form the paracellular barrier in epithelia. Claudins are ~22 kDa proteins that were first identified by Mikio Furuse in the laboratory of the late Shoichiro Tsukita as proteins that copurified in a tight junction fraction from the chicken liver [23]. The observation that they were transmembrane proteins with 4 predicted membrane domains and 2 extracellular domains raised early on the possibility that they could play a key role in intercellular adhesion and formation of the paracellular barrier. In 1999, Richard Lifton's group identified mutations in a novel gene, which they called paracellin, as the cause of familial hypercalciuric hypomagnesemia, an inherited disorder believed to be due to failure of paracellular reabsorption of divalent cations in the thick ascending limb of the renal tubule [78]. Paracellin turned out to be a claudin family member (claudin-16). This suggested that claudins in general might be directly involved in regulating paracellular transport in all epithelia. This is now supported by numerous studies demonstrating that overexpressing or ablating expression of various claudin isoforms in cultured cell lines or in mice affects both the degree of paracellular permeability and its selectivity (*vide infra*). Furthermore, in mammals alone there are ~24 claudin genes and each exhibits a distinct tissue-specific, pattern of expression. Thus, the specific claudin isoform(s) expressed in each tissue might explain its paracellular permeability properties.

Expression of many, but not all, of the claudins have been mapped along the renal tubule, predominantly by immunostaining of fixed tissues from various species (Fig. 1). Along the

renal tubule, each nephron segment expresses a unique set of multiple claudin isoforms, and each isoform is expressed in multiple segments, thus making a complicated picture which even varies between different species. The role of combinations of claudins in determining paracellular permeability properties has hardly been studied yet (see, e.g. [37]). In mouse, rabbit and cattle, the thick ascending limb of Henle's loop is thought to express claudins 3, 10, 11, 16 [46,50,78,85] in adulthood, and, at least in mouse, additionally claudin-6 during development [1]. In addition, claudin-4 has been found in cattle [65] and claudin-8 in rabbit [29]. To date, the distribution of Claudin-19 has been investigated in mouse, rat, and man where its presence in the TAL was demonstrated [5,50,54].

PARACELLULAR TRANSPORT IN THE TAL

Generation of the lumen-positive electrical potential

The thick ascending limb (TAL) of Henle's loop, working as "diluting segment" of the nephron, is characterized by two major properties: high transepithelial, resorptive transport of electrolytes and low permeability to water. Major players to achieve electrolyte transport are the apical $\text{Na}^+\text{-K}^+\text{-2Cl}^-$ symporter (NKCC2), the apical K^+ channel ROMK, the basolateral Cl^- channel (CLC-Kb) together with its subunit barttin and the basolateral $\text{Na}^+\text{/K}^+\text{-ATPase}$ (Fig. 2). The combined actions of these transport systems have been extensively reviewed (see e.g. [38,47,49,52,53]) and are therefore only briefly summarized here. Na^+ and Cl^- are resorbed by entering the cells apically through NKCC2 and leaving the cells basolaterally through the $\text{Na}^+\text{/K}^+\text{-ATPase}$ and CLC-Kb, respectively. In contrast, K^+ is either recycled across the apical membrane as it is entering through NKCC2 and leaving through ROMK, or even secreted, as it is also entering the cells basolaterally through the $\text{Na}^+\text{/K}^+\text{-ATPase}$. Taking these ion movements together, there is a net movement of positive charge from the basolateral to the apical side of the epithelium, giving rise to a lumen positive voltage (3 – 9 mV [11]; about 5 – 7 mV [30,31]; 7 – 8 mV [57]). Over the length of the TAL, luminal NaCl concentration decreases gradually to concentrations of 30 – 60 mM at the transition to the distal tubule [10], depending on the flow rate within the tubule (low flow rates resulting in low concentrations).

To keep up such a high gradient, the TAL epithelium has to be tight to water and various studies summarized by Burg and Good [10] report water permeability values from 28 $\mu\text{m/s}$ down to values indistinguishable from zero. Tight junctions of the TAL are, however, highly permeable to cations with P_{Na} being about 2 – 2.7 fold [11], 2.5 fold [30] or even up to 6 fold [10] that of P_{Cl} . Amongst the monovalent cations, a permeability sequence of $P_{\text{K}} > P_{\text{Na}} > P_{\text{Rb}} = P_{\text{Li}} > P_{\text{Cs}} > P_{\text{organic cation}}$ was observed [30] which is similar to Eisenman sequence VIII or IX [18], indicating a strong interaction between the permeating ion and the paracellular pore that enables at least partial removal of the hydration shell (see below). As reviewed by Burg and Good [10], the transepithelial sodium and chloride permeabilities, estimated from radioisotope fluxes, are high (in the range of $10 - 63 \cdot 10^{-6} \text{ cm/s}$) and the transepithelial electrical resistance is correspondingly low (21 – 25 W cm^2 [11]; 30 – 40 W cm^2 [31]; 11 – 34 W cm^2 [10]). Blocking active transport by the application of furosemide or ouabain increases transepithelial resistance only slightly, indicating that the low values are primarily due to a very high paracellular permeability [30].

Due to these properties of TAL epithelial cells, Na^+ ions leak back into the lumen of the tubule, creating a diffusion (dilution) potential that adds another 10 – 15 mV to the lumen positive potential [31], so that considerable potential differences (25 mV [10]; 30 mV [11], [30]; cTAL 23 mV, mTAL 17 mV [57]) may be reached at very slow flow rates.

Mechanism of Ca^{2+} and Mg^{2+} transport

Considerable proportions of the initially filtrated Mg^{2+} (50 – 60% [16]; 50 – 70% [73]; 65 – 75% [13]) and Ca^{2+} (20% [33]; 30 – 35% [16]) are resorbed in the TAL. The transepithelial potential is considered to provide the driving force for the predominantly paracellular resorption of Mg^{2+} and Ca^{2+} (for review see [13,16,73,74]) as in many studies, transport of both divalent ions in the TAL has been found to be strictly voltage dependent (resorptive at lumen positive potentials, zero at 0 mV and secretory at lumen negative potentials [9,17]) and permeability considerable ($\text{PCa } 7.7 \cdot 10^{-6}$ cm/s, i.e. approximately 25% of PNa [9]). There is however, some conflicting evidence, e.g. by Suki et al. [81] and Friedman [20]. Both studies used cTAL (cortical TAL) and found that decreasing the transepithelial potential by applying furosemide did either not alter the unidirectional lumen to bath Ca^{2+} flux (rabbit [81]) or left a substantial net Ca^{2+} resorption (mouse [20]). Similarly, Rocha et al. [70] found that bath application of ouabain almost abolished the transepithelial potential, but hardly affected net Ca^{2+} resorption and conclude that (a) all segments of Henle's loop are relatively impermeable to calcium and (b) net calcium resorption occurs in the thick ascending limb which cannot be explained by passive mechanisms.

The situation is further complicated by species-specific differences in divalent cation resorption. Mandon et al. [57] conclude that both Mg^{2+} and Ca^{2+} are transported in the cTAL but not in the mTAL (medullary TAL) of rat and mouse, although transepithelial potential differences were similar in both segments, and even if the transepithelial potential was experimentally elevated to values above 20 mV. Wittner et al. [92] even found evidence that in mouse mTAL the passive permeability to divalent cations is very low and that Ca^{2+} and Mg^{2+} can be secreted into the luminal fluid under conditions which elicit large lumen-positive transepithelial potential differences. They conclude that this Ca^{2+} and Mg^{2+} transport is most probably of cellular origin. In contrast, in rabbit, both ions are transported along the whole length of the TAL ([57], for review see [16]).

Both, Mg^{2+} and Ca^{2+} resorption are modulated through the action of the basolateral Ca (and Mg) sensing receptor (CaSR) which is found along the entire nephron but especially in the loop of Henle, distal convoluted tubule (DCT) and the inner medullary collecting duct [15]. Different modes of action on Ca^{2+} and Mg^{2+} homeostasis exist, such as an indirect action through the modulation of PTH secretion or direct effects on the cells expressing CaSR. In the TAL the latter model is based on the assumptions depicted above, i.e. that Mg^{2+} and Ca^{2+} are resorbed paracellularly, driven by the lumen positive potential, so that a reduction in NaCl resorption causes a reduction in driving force for Mg^{2+} and Ca^{2+} resorption. As reviewed by Hebert [33] and Ward [87], CaSR is activated through an increase in basolateral Ca^{2+} and/or Mg^{2+} concentration which triggers an increase in the intracellular Ca^{2+} concentration. This reduces the activity of the adenylate cyclase which, in turn, inhibits transcellular transport of Na^+ and Cl^- . In addition, the increase in intracellular Ca^{2+} activates phospholipase A2 (PLA2) and thus increases the intracellular concentration of arachidonic acid and its derivative, 20-HETE. 20-HETE inhibits NKCC2, ROMK and the Na^+/K^+ -ATPase and by this Mg^{2+} and Ca^{2+} resorption (Fig. 2). In keeping with this hypothesis, mutations in CaSR affect Ca/Mg resorption (for review see [13,60,74]). Inactivating mutations cause hypercalcemia, hypocalciuria, hypomagnesiuria and, in some patients hypermagnesemia. Conversely, activating mutations (gain of function mutations) lead to hypocalcemia, hypercalciuria, hypermagnesiuria and in up to 50% of the patients mild hypomagnesemia [13,53,60].

Insights from Bartter syndrome

While defects in CaSR indirectly affect many of the transporters involved in the production of the lumen-positive potential in the TAL, the group of mutations subsumed as Bartter syndrome affect single compounds (for rev. see e.g. [13,47,71,74]). The effect on Mg^{2+} -homeostasis is

variable: Bartter syndrome type I (mutations in NKCC2), and type II (mutations in ROMK) lead to hypercalciuria and thus cause nephrocalcinosis [47], but no hypomagnesemia is observed [53]. Reports on hypermagnesiuria are conflicting: while Kleta and Bockenhauer [47] link it to nephrocalcinosis seen in these patients, Rodriguez-Soriano [71] states that patients with neonatal Bartter syndrome (i.e. type I or II) show a lack of hypermagnesiuria that may be explained by compensation in the DCT. Hypomagnesemia is occasionally present in Bartter type III (CLC-Kb). However, here it is believed to be mainly due to effects on DCT, where CLC-Kb shows highest expression [52]. Patients with Bartter syndrome IV (CLC-Ksubunit barttin) may [53] or may not [47] present nephrocalcinosis, while Mg^{2+} homeostasis appears undisturbed. Interestingly, the largest effects on Mg^{2+} -homeostasis are observed in Gitelman syndrome [26], a defect in the Na^+/Cl^- symport (NCC) predominantly found in the DCT, where Mg^{2+} is transported along the transcellular route [13]. Affected patients suffer from hypomagnesemia, hypermagnesiuria and hypocalciuria [53]. The effect on Mg^{2+} in Gitelman syndrome is still poorly understood and possibly due to a concomitant down-regulation of TRPM6, the apical Mg^{2+} uptake channel in DCT [47].

ROLE OF TAL CLAUDINS IN FAMILIAL HYPERCALCIURIC HYPOMAGNESEMIA WITH NEPHROCALCINOSIS (FHHNC)

Clinical features and genetics of FHHNC

FHHNC is a rare autosomal recessive disease that is characterized by renal Mg^{2+} and Ca^{2+} wasting [69]. Patients present with complications of hypomagnesemia such as tetany and seizures, and develop nephrocalcinosis and progressive renal insufficiency [72]. FHHNC is distinct from Gitelman's syndrome because the patients do not generally have salt wasting, hypokalemia and metabolic alkalosis [26]. Rodriguez-Soriano first proposed that FHHNC might be due to a defect in tubular reabsorption in the TAL [72]. This was based on the magnitude of the observed increase in fractional excretion of Mg^{2+} , which could only be accounted for by a defect in the TAL, and on the fact that linked transport of Ca^{2+} and Mg^{2+} is characteristic of the TAL. Blanchard *et al.* [8] subsequently demonstrated that FHHNC patients are unable to further increase their fractional excretion of Mg^{2+} and Ca^{2+} in response to the loop diuretic, furosemide, while having a preserved natriuretic response, thus confirming that there is a selective defect in divalent cation reabsorption in the TAL.

More than 30 different claudin-16 mutations have now been reported in families with FHHNC [62,63,89,90]. Because of the large number of unique mutations, it has not been possible to identify any clear qualitative correlation between the phenotype and individual mutations, although certain mutations are associated with greater severity of disease [51]. In 2006, a second locus was identified, CLDN19, which encodes claudin-19 [50]. In the initial report, the phenotype appeared similar to that due to claudin-16 mutations, with the exception that there was a high prevalence of ocular abnormalities, including macular colobomata, nystagmus and myopia. Claudin-19 is normally expressed at high levels in the retina [50], but why it causes these ocular disorders is unknown.

In vitro studies of claudin permeability: function of claudins 16 and 19

In vitro studies of claudin function comprise inducible or non-inducible transfection of various cells lines with cDNA for claudins that are not endogenously expressed by the cell line used. Alternatively, cells can be transfected with siRNA directed against an endogenous claudin. In both cases, cells are then grown to confluence on permeable filter supports that allow measurement of transepithelial permeabilities. Before the results of permeability studies can be interpreted, however, several parameters have to be controlled. First, special care has to be taken to make sure that the exogenous claudin is correctly inserted into the tight junction. This can be achieved e.g. by confocal laser scanning microscopy, colocalizing the claudin of interest

with a tight junction marker protein such as occludin. Second, it has to be ensured that endogenous claudin expression remains unaffected, as permeability changes always result from the combined effects of alterations in endogenous and exogenous claudins [6]. Third, it has to be kept in mind that, typically, epithelia express several different claudins that act together to produce tissue specific permeability properties. Thus, ideally, a cell line should be chosen that provides a claudin background resembling that usually experienced by the claudin investigated. The latter two points may be the reason for contradicting results obtained in permeability studies expressing a specific claudin in different cell lines (reviewed by [4]).

Studies of paracellular permeabilities can be divided into two groups, those employing electrophysiological measurements (e.g. determination of diffusion potentials), and those measuring ion or solute flux, using either radioactive isotopes or various analytical methods to determine the amount transported. As discussed below, all these techniques have their specific methodological advantages and drawbacks (for summary see Table I).

Electrophysiological Methods—A direct approach to determine relative permeabilities (e.g. P_{Na}/P_{Cl}) of epithelia or cell layers is the determination of diffusion potentials caused by the application of different solutions on the apical and basolateral side of the epithelium. If, in addition, the transepithelial conductance is known, absolute permeabilities can be calculated using the Kimizuka-Koketsu equation ([45], for a simplified equation see e.g. [5,35]). Most common difficulties encountered with this technique are due to active responses of the tissue to the change in bath solutions, i.e. activation of an electrogenic, transcellular transport pathway that causes changes in the transepithelial potential which add onto the diffusion potential. Many of these transport pathways may be blocked by using K^+ -free bath solutions to block the Na^+/K^+ -ATPase. However, this, in turn, may lead to cell swelling [42] and thus to a decrease in paracellular space that blocks the paracellular transport investigated. Most common technical difficulties arise from differences in ionic strength of the bath solutions used and thus in the single ion activity coefficients of the ions investigated, which cannot be precisely calculated in complex solutions. Furthermore, changing the composition of the bath solution during the experiments may give rise to liquid junction potentials at the interface of the bath solution and the agar bridge used for connection to the voltmeter. These potentials may well be in the order of the diffusion potential expected to be measured across the epithelium.

Although transepithelial conductances depend on paracellular permeabilities of the predominant ions in the bath solution, conductance changes alone cannot be used to predict ion permeabilities. Firstly, conductances always depend on both ion and counter-ion, not on one ion species alone. Secondly, transepithelial conductances are the sum of the conductances of the transcellular and paracellular pathways. Thus, they only reflect paracellular permeability, if paracellular conductance dominates transepithelial conductance and if transcellular conductance remains constant throughout the experiment. This, however, is often not the case, as concentration changes of the ions investigated may affect transcellular conductance, e.g. by activating ion transporters or by inhibiting ion channels. Thirdly, the specific conductance of each solution employed may differ and has therefore to be assessed and taken into account. Thus, comparison of results from diffusion potential measurements or flux studies and conductance measurements may even yield contradicting results [82,93]. For the same reasons, other methods based on pure conductance/resistance measurements, including the more sophisticated conductance scanning method [27,48] or one-path impedance spectroscopy [21,22,27] are not ion specific and do not allow the measurement of paracellular permeabilities to single ions.

Flux measurements—In contrast to electrophysiological measurements, flux measurements are not limited to ions but can also be extended to uncharged molecules. If radioisotopes or labelled compounds (radioactive, fluorescence) are used, uni-directional fluxes can

be determined under steady-state conditions, i.e. with equal total concentrations of the (unlabelled) compound on both sides of the epithelium. The tracer is added to the donor-side at such low concentration that the resulting concentration gradient is insignificant. If no labelling is possible or radio-isotopes are not readily available, flux has to be measured under “zero - trans” conditions, i.e. the compound to be investigated is added only to the donor (“cis”) side of the epithelium, the initial concentration on the acceptor (“trans”) side is zero. Increases in concentration on the trans-side are measured employing appropriate analytical methods (e.g. atomic absorption spectroscopy, electron probe spectroscopy, mass spectroscopy, HPLC, fluorimetric measurements, ion-selective electrodes etc.). As transport kinetics under steady-state conditions and zero - trans conditions differ, results obtained under these two conditions may not be comparable [79].

Flux measurements per se do not distinguish between transcellular or paracellular transport. Therefore, to estimate paracellular permeabilities, inhibition or at least estimation of the transcellular flux is necessary. Assuming that transcellular flux for energetic reasons is not easily reversible while paracellular flux is passive and thus generally assumed to be symmetric, the transcellular proportion is often estimated by calculating the difference between apical to basolateral and basolateral to apical fluxes. Care has also to be taken, that experimental conditions do not change the permeability of the pathway investigated (e.g. by inducing cell volume changes or by affecting tight junction integrity).

All flux measurements are very sensitive to the development of diffusion zones (“unstirred layers”) near the cells. These layers are depleted/enriched in the compound transported and thus alter the driving forces acting on these compounds, if bath solutions are not continually circulated. If ionic fluxes are investigated, transepithelial potentials may develop that diminish or completely inhibit the flux investigated. These can be compensated for in an Ussing-chamber set-up that keeps the bath solution in constant motion and allows to clamp the transepithelial voltage to zero.

All the techniques described above have been employed to investigate the function of claudin-16 and -19, especially with respect to their ability to increase paracellular permeability to divalent cations. The hypothesis, that claudin-16 (then called paracellin-1) may be a paracellular Mg^{2+} and Ca^{2+} pore was originally expressed by Simon et al. [78]. It was based on the findings that mutations in claudin-16 were the cause of the severe disturbance in Mg^{2+} and Ca^{2+} homeostasis in FHHNC patients together with the observations that claudin-16 is a tight junction protein located in the TAL, i.e. the nephron segment responsible for bulk Mg^{2+} reabsorption along the paracellular pathway. When, recently, it was found that claudin-19 mutations were underlying hitherto unexplained cases of FHHNC and that claudin-19 co-localized with claudin-16, the hypothesis was extended to claudin-19 [50].

The Mg^{2+} / Ca^{2+} pore hypothesis was put to a direct test in a number of *in vitro* studies investigating the effects of claudin-16 and -19 transfection on paracellular Mg^{2+} and Ca^{2+} permeability. However, data from these studies are conflicting and if increases in Mg^{2+} and Ca^{2+} permeabilities were observed, these effects were so small, that it appeared doubtful whether they could explain the dramatic disturbances in Mg^{2+} homeostasis observed in FHHNC. One major source of variability in these transfection studies is the choice of the epithelial cell line (e.g. high resistance, cation-prefering MDCK-C7 cells; low resistance, highly cation-selective MDCK-II cells; low-resistance, anion-selective LLC-PK1 cells). All these cell lines are characterized by their own set of endogenous claudins that may interact with the exogenous claudins and thus dominate the observed effects [84]. Ikari et al. [39,40] transfected low resistance MDCK cells with claudin-16 and reported that Ca^{2+} flux in these cells was increased in the apical to basolateral direction while Ca^{2+} flux in the opposite direction remained unchanged. The apical to basolateral flux was competitively inhibited by Mg^{2+} ,

which was taken as indirect evidence for an increased Mg^{2+} permeability. In spite of increased Ca^{2+} and Mg^{2+} permeabilities, claudin-16 expression caused an increase in transepithelial resistance in these cells, possibly due to a concomitant decrease in Na^+ permeability.

The asymmetry of Ca^{2+} flux remains unexplained. It might be due to active, transcellular Ca^{2+} transport in the apical to basolateral direction, that would somehow have to be linked to the expression of claudin-16. It might also be due to the method employed in this study. Although Ca^{2+} flux was measured with the radioactive isotope ^{45}Ca as a tracer, experiments were not carried out under steady-state but under zero - trans conditions. However, tight junctions are known to be sensitive to the withdrawal of extracellular Ca^{2+} [59] which leads to their disintegration and this may have affected the outcome of the flux measurements.

Alternatively, the asymmetry of Ca^{2+} flux may be explained by recent findings of the same group [41] that CaSR activation by basolateral Ca^{2+} or Mg^{2+} leads to removal of claudin-16 from the tight junction due to PKA inhibition. The underlying mechanism is a reduction in Ser217 phosphorylation of claudin-16 which had previously been found to be essential for its localization in the tight junction [40].

In contrast to these studies, Hou et al. [35] found an only moderately enhanced Mg^{2+} permeability without directional preference in LLC-PK1 cells, accompanied by a large increase in Na^+ permeability. This increase in P_{Na} was greatly reduced or completely absent in all FHHNC relevant claudin-16 mutants investigated. In the inherently cation-selective MDCK-II cells, Hou et al. [35] found no significant effects of claudin-16 on P_{Na} , P_{Cl} or P_{Mg} . Because of the comparatively small increase in P_{Mg} relative to the permeability changes for monovalent cations, Hou et al. [35] conclude that the Mg^{2+} -pore hypothesis for claudin-16 is not valid. They put forward the hypothesis that FHHNC is caused by a reduction in transepithelial potential due to the decreased P_{Na} observed in the presence of mutated claudin-16.

While Ikari et al. [39–41] and Hou et al. [35] used low resistance cell lines, Kausalya et al. [43] employed the high-resistance MDCK-C7 cell line in their transfection studies. They found a moderately increased Mg^{2+} permeability (without directional preference) in claudin-16-transfected cell layers, compared to mock-transfected controls and cells transfected with various claudin-16 mutants. No correlation between Mg^{2+} permeability and transepithelial resistance was detected and neither P_{Na} nor P_{Cl} were affected by claudin-16 transfection.

Thus, the only consistent effect in the different cell lines transfected with claudin-16 is the increase, albeit small, in P_{Mg} . Considering the dramatic effect of mutations in claudin-16 on Mg^{2+} and Ca^{2+} homeostasis in FHHNC patients, the effect of claudin-16 on P_{Mg} appears so small that the mechanism of how claudin-16 enhances Mg^{2+} resorption is still far from being clear.

To date, only two *in vitro* studies on claudin-19 have been published, namely Angelow et al. [5], using mouse claudin-19 variant 2 and Hou et al. [37], using human claudin-19 variant 2. Angelow et al. [5] stably transfected low resistance MDCK-II cells using a TetOff system and found a claudin-19 induced increase in transepithelial resistance together with a decreased paracellular permeability to mono- and divalent cations. Permeability to Cl^- remained unaltered. They thus conclude that claudin-19 acts as a paracellular cation barrier.

Hou et al [37] used MDCK-II and LLC-PK1 cells transfected with claudin-19 alone or together with claudin-16. They found an increase in transepithelial resistance together with a decreased paracellular permeability to Cl^- in LLC-PK1 cells without concomitant effect on P_{Na} . P_{Mg} was slightly but significantly decreased. However, they failed to reproduce the claudin-19 effect in MDCK-II cells observed by Angelow et al. [5]. This may be due to a species difference (mouse

vs. human claudin-19) or to the fact that the TetOff system used by Angelow et al. [5] allows a more direct comparability between induced and non-induced cells.

When co-expressing claudin-16 and claudin-19 in LLC-PK1 cells, Hou et al. [37] found additive effects: the claudin-16 induced increase in P_{Na} together with the claudin-19 induced decrease in P_{Cl} caused further increase in the P_{Na}/P_{Cl} ratio, the prerequisite for the formation of the large diffusion potentials in the TAL described above.

Lessons from animal models of FHHNC

Claudin-16 defects are known to be the cause of a hereditary disease in Japanese Black Cattle [34,66]. This autosomal recessive disorder is known as “bovine chronic interstitial nephritis with diffuse zonal fibrosis” (CINF) or “renal tubular dysplasia in Japanese Black cattle”. In contrast to FHHNC it is not only characterized by the absence of claudin-16 from the TAL but in addition by a reduction in the number of glomeruli, glomerular and tubular atrophy, interstitial fibrosis and lymphocytic infiltration [66], increased blood urea nitrogen, creatinine, and urinary protein levels as well as decreased serum calcium [34]. Effects on serum magnesium levels were variable and could be increased, decreased or unchanged [66]. Thus, cattle affected by claudin-16 defects present a completely different disease from FHHNC, that involves not only ion resorption but also glomerular filtration [34] and cannot, therefore be used as a model of FHHNC. The cause underlying the observed differences between CINF and FHHNC are not yet clear.

The only mouse model of FHHNC so far was generated by Hou *et al.* [36]. They used lentiviral transgenesis of shRNA to knock down claudin-16 expression by >99% in mouse kidneys. Claudin-16 knockdown mice had hypomagnesemia with ~4-fold increase in the fractional excretions of both Ca^{2+} and Mg^{2+} . The fact that knock down of claudin-16 reproduces the FHHNC phenotype confirms that the human disease is due to loss-of-function mutations in claudin-16.

As discussed above (Fig. 2), the paracellular reabsorption of cations is normally driven by a lumen-positive voltage (V_{te}) that is generated by transcellular Na^+ reabsorption in two ways: (a) electrogenic transcellular transport due to apical K^+ recycling (blockable by furosemide), and (b) generation of a diffusion potential due to build-up of a transtubular $NaCl$ gradient. When isolated TAL segments were perfused *in vitro* with symmetrical $NaCl$ solutions, there was no difference in V_{te} between knockdown and control mice. Thus component "a" was generated normally. However, in the presence of furosemide, P_{Na}/P_{Cl} was significantly reduced from 3.1 ± 0.3 in wild-type animals to 1.5 ± 0.1 in the knockdown mice. P_{Na}/P_{Mg} , as measured by biionic potentials, was unchanged, suggesting that there was a non-specific reduction in cation permeability. This would be predicted to substantially reduce the component of the transepithelial voltage that is due to the $NaCl$ diffusion potential (component "b"). For example, with asymmetric $NaCl$ concentrations of 145 mM and 30 mM, the corresponding diffusion potential was 18 mV in wild-type mice, but only 6.6 mV in the knockdown mice. Insofar as the lumen-positive voltage normally provides the driving force for divalent cation reabsorption in the TAL under physiological conditions, a reduction in this potential could well be the explanation for the Ca^{2+} and Mg^{2+} wasting observed in these mice.

It is interesting to consider what would be the predicted effect on TAL Na^+ handling. Component "a" of V_{te} (unlike component "b") drives not only paracellular reabsorption of divalent cations, but also of Na^+ and this route contributes significantly to total TAL Na^+ reabsorption. Thus, if P_{Na} is reduced, overall reabsorption of Na^+ by the TAL should be reduced. Indeed, claudin-16 knockdown mice had increased fractional excretion of Na^+ . They were also hypotensive and had elevated plasma aldosterone levels, suggesting that they may have been total body Na^+ -depleted. Furthermore, they had a 27% reduction in glomerular

filtration rate (GFR), were hypokalemic, and had moderately increased fractional excretion of K^+ . The reduction in GFR could be due to increased NaCl delivery from the medullary and early cortical TAL to the macula densa, activating tubuloglomerular feedback, or to reduction in blood pressure below the autoregulatory range. Increased delivery of Na^+ out of the TAL, together with elevated aldosterone levels, would also be predicted to increase electrogenic Na^+ reabsorption in the connecting tubule and collecting duct. This would enhance K^+ secretion in these segments, thus explaining the renal K^+ wasting and hypokalemia. Thus, all the findings in the claudin-16 knockdown mice support the premise that claudin-16 behaves as a non-specific cation channel and that loss of TAL Na^+ permeability is the predominant problem responsible for the disease phenotype.

Several discrepancies between data from FHHNC patients and the present models remain. Thus, the abnormalities in Na^+ and K^+ handling in claudin-16 knockdown mice (which resemble a Bartter's phenotype) are not found at all in human patients with FHHNC. Moreover, Blanchard's studies in humans with FHHNC showed that fractional excretion of Na^+ was normal at baseline and increased normally in response to furosemide [8]. Furthermore, Bartter syndrome, which also affects the driving force for Mg^{2+} reabsorption, primarily by acting on component "a" of V_{te} , is only rarely associated with hypomagnesemia. As mentioned above, Bartter type III is the only Bartter type in which hypomagnesemia is occasionally present, but believed to be mainly due to effects on DCT [52], the same location that is affected by Gitelman syndrome which is associated with much more severe hypomagnesemia. It should, therefore, be kept in mind that at least part of FHHNC may result from disturbances in the DCT. Unfortunately data on claudin-16 and -19 expression in this nephron segment are conflicting. Simon et al. [78] detected claudin-16 mRNA in the DCT of rat kidney, and Weber et al. [91] report its presence in DCT based on immunohistochemical staining of rat kidney tissue. In contrast, in their study on mouse tissue, Kiuchi-Saishin et al. [46] found claudin-16 exclusively in the TAL. Similarly, claudin-19 was described to be present in DCT and collecting duct and only to a lesser extent in TAL of mouse, rat and human kidneys by Lee et al. [54] while the reverse was observed in mouse by Konrad et al. [50]. Thus, mice may not be perfect models of the human disease.

MECHANISMS OF ION PERMEATION THROUGH CLAUDINS

Freeze fracture studies show that tight junctions are organized in an elaborate network of protein strands. In many tissues, the number of horizontal strands, the complexity and the intactness of these strands correlate with the tightness of the epithelium [12,56], although this correlation does not hold generally [25,61,80]. It is noteworthy, however, that under several pathological conditions barrier function and tight junction strand complexity are altered simultaneously [75,77,94]. Exogenous expression of claudins may introduce specific changes in strand formation, such as a "pearl string" appearance or small gaps along single strands. However, the exact organization of tight junction proteins within these strands is not yet clear.

Current models of paracellular pore formation assume that there are homo- and heteromeric interactions between claudins both within the same membrane (cis interaction) and between the extracellular loops of claudins from two neighbouring cells (trans interaction [4,24,25,68]). However, interactions do not occur between any two claudins. For example, claudin-1 has been found to interact with claudin-4 but not with claudin-2 [25]. Similarly, in a coimmunoprecipitations study, Hou et al. [37] found direct interactions between claudin-16 and -19, but not between claudin-16 and claudin-2. Furthermore, Hou et al. [37] were able to demonstrate in yeast and mouse L-cells, that claudin-19 but not claudin-16 is able to form homomers. Formation of claudin-16/claudin-19 heteromers and of claudin-19 homomers was affected by various claudin-16 and claudin-19 mutations relevant to FHHNC.

Functional studies show that there have to be at least two types of paracellular pores, distinguishing either between charged and uncharged solutes and/or according to size. Thus, Amasheh et al. [2] found an increase in cation permeability upon claudin-2 transfection of MDCK-C7 cells which caused a dramatic decrease in transepithelial resistance but which was not accompanied by an increase in mannitol flux. Thus, the pore created by claudin-2 was large enough to let Na^+ pass, but it was charge selective, as it was able to exclude Cl^- , as well as it was size selective, as it also excluded mannitol. Anderson et al. [3] therefore suggested a model in which ions passed the tight junction through a continuous row of small pores while larger solutes pass consecutively through gaps in tight junctions strands that dynamically open and close over time.

Independent of any underlying model, the existence of two types of paracellular permeation pathways has been demonstrated in two intriguing studies, employing a multitude of PEG oligomers with molecular radii between about 3 and 7 Å [86,88]. In both studies, permeability could be described by two components: a high capacity pathway with an estimated pore radius of about 4 Å and a low capacity pathway with a pore radius of at least 7 Å. Most physiologically relevant inorganic ions should thus be able to pass through the high capacity pathway, even when hydrated, possibly with the exception of Mg^{2+} which has a hydrated radius of 4.28 Å [64] and is thus larger than glucose ($r = 3.8$ Å [67]) and of similar size as mannitol ($r = 4.2$ Å [76]). It can therefore be assumed that the high capacity pathway dominates paracellular conductance.

The high capacity pathway acts like a channel rather than a carrier mechanism, as it is only mildly temperature dependent [82]. Only the high resistance MDCK-I cells showed a stronger temperature dependence in this study. This may indicate that these cells contain so few small pores that here the low capacity, large radius pathway plays a more dominant role and that this pathway may indeed depend on structural changes as suggested by Anderson et al [3].

Diffusion potential studies comparing permeabilities of different monovalent cations result in permeability sequences corresponding to high order Eisenman sequences (IV, changing to X upon claudin-10b expression [32]; VIII or IX [30]; IIIV and X, depending on cell type [82]; XI [35]), indicating the presence of a strong field-strength binding site within the paracellular pore that enables at least partial removal of the hydration shell. This view is supported by the observation, that titration of the negative charges at pH values of about 4 changes the permeability sequence to Eisenman sequence I [82]. If more than one ion cation species is present, relative permeabilities shift due to exclusion effects at the pore [82]. From this the authors conclude that different ions compete for occupancy within the pore.

Structure-function studies of claudins indicate that the electrical charges responsible for the paracellular selectivity filter reside within the first extracellular loop of the claudins [3,4,14, 35,83,85]. As already mentioned, the hydrated Mg^{2+} is too large to pass the small, high capacity pores of the tight junction. This is in keeping with the findings by Tang and Goodenough [82] who find an unexpectedly low permeability for Mg^{2+} in MDCK-II cells, in which the paracellular pathway is dominated by this high capacity pathway. Mg^{2+} substitutes its inner sphere water molecules at a rate about 1000 times more slowly than Ca^{2+} [58]. Consequently, a Mg^{2+} pore must involve a large initial binding site and/or more elaborate means of dehydration than are commonly found for other cations [44]. Due to its highly charged first extracellular loop (10 negative and 6 positive charges) which differs considerably from the first extracellular loops of all other claudins, claudin-16 appeared to fulfill this requirement. Hou et al. [35] mutated the charged amino acids of the first extracellular loop of claudin-16 and found strong effects on the claudin-16 induced increase in paracellular Na^+ permeability. It is noteworthy, however, that none of the negative charges are mutated in FHHNC patients, so that the relevance of the findings by Hou et al. [35] is not yet clear. Moreover, claudin-19,

which is also connected to Mg^{2+} transport, contains only 4 negative and 4 positive charges within its first extracellular loop, and bears high homology to many other claudins.

CONCLUSIONS

In summary, the paracellular pathway in the TAL is an important route for renal reabsorption of Na^+ , Ca^{2+} and Mg^{2+} . We now know of the existence of at least 5 different claudin isoforms that are expressed in this nephron segment and could play a role in determining paracellular permeability. Mutations in two of these, claudin-16 and claudin-19 affect renal Ca^{2+} and Mg^{2+} handling in the human disease, FHHNC. Mice with knockdown of claudin-16 reproduce features of the human disease but also have renal Na^+ wasting, and support a model in which claudins 16 and 19 determine paracellular Na permeability. Charged residues in the first extracellular loop of these claudins probably determine their permeability properties, but their precise role remains to be fully elucidated. Finally, it would be of interest to investigate the potential involvement of the DCT in the generation of FHHNC.

ACKNOWLEDGEMENTS

Work from our own groups that is cited here was supported by German Research Foundation grant GU447/11-1 (to D.G.) and National Institutes of Health grant DK062283 (to A.Y.).

REFERENCES

1. Abuazza G, Becker A, Williams SS, et al. Claudins 6, 9, and 13 are developmentally expressed renal tight junction proteins. *Am J Physiol Renal Physiol* 2006;291:F1132–F1141. [PubMed: 16774906]
2. Amasheh S, Meiri N, Gitter AH, et al. Claudin-2 expression induces cation-selective channels in tight junctions of epithelial cells. *J Cell Sci* 2002;115:4969–4976. [PubMed: 12432083]
3. Anderson JM, Van Itallie CM, Fanning AS. Setting up a selective barrier at the apical junction complex. *Curr Opin Cell Biol* 2004;16:140–145. [PubMed: 15196556]
4. Angelow S, Yu ASL. Claudins and paracellular transport: an update. *Curr Opin Nephrol Hypertens* 2007;16:459–464. [PubMed: 17693762]
5. Angelow S, El-Husseini R, Kanzawa SA, et al. Renal localization and function of the tight junction protein, claudin-19. *Am J Physiol Renal Physiol* 2007;293:F166–F177. [PubMed: 17389678]
6. Angelow S, Schneeberger EE, Yu AS. Claudin-8 expression in renal epithelial cells augments the paracellular barrier by replacing endogenous claudin-2. *J Membr Biol* 2007;215:147–159. [PubMed: 17516019]
7. Ben-Yosef T, Belyantseva IA, Saunders TL, et al. Claudin 14 knockout mice, a model for autosomal recessive deafness DFNB29, are deaf due to cochlear hair cell degeneration. *Hum Mol Genet* 2003;12:2049–2061. [PubMed: 12913076]
8. Blanchard A, Jeunemaitre X, Coudol P, et al. Paracellin-1 is critical for magnesium and calcium reabsorption in the human thick ascending limb of Henle. *Kidney Int* 2001;59:2206–2215. [PubMed: 11380823]
9. Bourdeau JE, Burg MB. Voltage dependence of calcium transport in the thick ascending limb of Henle's loop. *Am J Physiol* 1979;236:F357–F364. [PubMed: 434209]
10. Burg M, Good D. Sodium chloride coupled transport in mammalian nephrons. *Annu. Rev. Physiol* 1983;45:533–547. [PubMed: 6342523]
11. Burg MB, Green N. Function of the thick ascending limb of Henle's loop. *Am. J. Physiol* 1973;224:659–668. [PubMed: 4691283]
12. Claude P, Goodenough DA. Fracture faces of zonulae occludentes from "tight" and "leaky" epithelia. *J Cell Biol* 1973;58:390–400. [PubMed: 4199658]
13. Cole DEC, Quamme GA. Inherited disorders of renal magnesium handling. *J Am Soc Nephrol* 2000;11:1937–1947. [PubMed: 11004227]

14. Colegio OR, Van Itallie CM, McCrea HJ, et al. Claudins create charge-selective channels in the paracellular pathway between epithelial cells. *Am J Physiol Cell Physiol* 2002;283:C142–C147. [PubMed: 12055082]
15. Dai L-J, Ritchie G, Kerstan D, et al. Magnesium transport in the renal distal convoluted tubule. *Physiol Rev* 2001;81:51–84. [PubMed: 11152754]
16. de Rouffignac C, Quamme G. Renal magnesium handling and its hormonal control. *Physiol Rev* 1994;74:305–322. [PubMed: 8171116]
17. Di Stefano A, Roinel N, de Rouffignac C, et al. Transepithelial Ca^{2+} and Mg^{2+} transport in the cortical thick ascending limb of Henle's loop of the mouse is a voltage-dependent process. *Ren Physiol Biochem* 1993;16:157–166. [PubMed: 7689239]
18. Eisenman G. Cation selective glass electrodes and their mode of operation. *Biophys J* 1962;2:259–323. [PubMed: 13889686]
19. Enck AH, Berger UV, Yu AS. Claudin-2 is selectively expressed in proximal nephron in mouse kidney. *Am J Physiol Renal Physiol* 2001;281:F966–F974. [PubMed: 11592954]
20. Friedman PA. Basal and hormone activated calcium absorption in mouse renal thick ascending limbs. *Am J Physiol* 1988;254:F62–F70. [PubMed: 2827519]
21. Fromm M, Palant CE, Bentzel CJ, et al. Protamine reversibly decreases paracellular cation permeability in *Necturus* gallbladder. *J Membr Biol* 1985;87:141–150. [PubMed: 4078883]
22. Fromm M, Schulzke JD, Hegel U. Epithelial and subepithelial contributions to transmural electrical resistance of intact rat jejunum, in vitro. *Pflügers Arch* 1985;405:400–402.
23. Furuse M, Fujita K, Hiragi T, et al. Claudin-1 and -2: novel integral membrane proteins localizing at tight junctions with no sequence similarity to occludin. *J Cell Biol* 1998;141:1539–1550. [PubMed: 9647647]
24. Furuse M, Sasaki H, Tsukita S. Manner of interaction of heterogeneous claudin species within and between tight junction strands. *J Cell Biol* 1999;147:891–903. [PubMed: 10562289]
25. Furuse M, Furuse K, Sasaki H, et al. Conversion of zonulae occludentes from tight to leaky strand type by introducing claudin-2 into Madin-Darby canine kidney I cells. *J Cell Biol* 2001;153:263–272. [PubMed: 11309408]
26. Gitelman HJ, Graham JB, Welt LG. A new familial disorder characterized by hypokalemia and hypomagnesemia. *Trans Assoc Am Physicians* 1966;79:221–235. [PubMed: 5929460]
27. Gitter AH, Bertog M, Schulzke JD, et al. Measurement of paracellular epithelial conductivity by conductance scanning. *Pflügers Arch* 1997;434:830–840.
28. Gitter AH, Schulzke JD, Sorgenfrei D, et al. Ussing chamber for high-frequency transmural impedance analysis of epithelial tissues. *J Biochem Biophys Meth* 1997;35:81–88. [PubMed: 9350514]
29. Gonzalez-Mariscal L, Namorado Mdel C, Martin D, et al. The tight junction proteins claudin-7 and -8 display a different subcellular localization at Henle's loops and collecting ducts of rabbit kidney. *Nephrol Dial Transplant* 2006;21:2391–2398. [PubMed: 16766545]
30. Greger R. Cation selectivity of the isolated perfused cortical thick ascending limb of Henle's loop of rabbit kidney. *Pflügers Arch* 1981;390:30–37.
31. Greger R. Chloride reabsorption in the rabbit cortical thick ascending limb of the loop of Henle. A Sodium Dependent Process. *Pflügers Arch* 1981;390:38–43.
32. Günzel D, Stuver M, Kausalya PJ, et al. Functional characterization of claudin-10 isoforms. *Acta Physiol* 2007;189:151.
33. Hebert SC. Calcium and salinity sensing by the thick ascending limb: a journey from mammals to fish and back again. *Kidney Int* 2004;66:S28–S33.
34. Hirano T, Kobayashi N, Itoh T, et al. Null mutation of PCLN-1/Claudin-16 results in bovine chronic interstitial nephritis. *Genome Res* 2000;10:659–663. [PubMed: 10810088]
35. Hou J, Paul DL, Goodenough DA. Paracellin-1 and the modulation of ion selectivity of tight junctions. *J Cell Sci* 2005;118:5109–5118. [PubMed: 16234325]
36. Hou J, Shan Q, Wang T, et al. Transgenic RNAi depletion of claudin-16 and the renal handling of magnesium. *J Biol Chem* 2007;282:17114–17122. [PubMed: 17442678]

37. Hou J, Renigunta A, Konrad M, et al. Claudin-16 and claudin-19 interact and form a cation-selective tight junction complex. *J Clin Invest* 2008;118:619–628. [PubMed: 18188451]
38. Huang C, Miller RT. Regulation of renal ion transport by the calcium-sensing receptor: an update. *Curr Opin Nephrol Hypertens* 2007;16:437–443. [PubMed: 17693759]
39. Ikari A, Hirai N, Shiroma M, et al. Association of paracellin-1 with ZO-1 augments the reabsorption of divalent cations in renal epithelial cells. *J Biol Chem* 2004;279:54826–54832. [PubMed: 15496416]
40. Ikari A, Matsumoto S, Harada H, et al. Phosphorylation of paracellin-1 at Ser217 by protein kinase A is essential for localization in tight junctions. *J Cell Sci* 2006;119:1781–1789. [PubMed: 16608877]
41. Ikari A, Okude C, Sawada H, et al. Activation of a polyvalent cation-sensing receptor decreases magnesium transport via claudin-16. *Biochim Biophys Acta* 2008;1778:283–290. [PubMed: 17976367]
42. Jensen PK, Fisher RS, Spring KR. Feedback inhibition of NaCl entry in *Necturus* gallbladder epithelial cells. *J Membrane Biol* 1984;82:95–104. [PubMed: 6502701]
43. Kausalya PJ, Amasheh S, Günzel D, et al. Disease-associated mutations affect intracellular traffic and paracellular Mg²⁺ transport function of claudin-16. *J Clin Invest* 2006;116:878–891. [PubMed: 16528408]
44. Kehres DG, Maguire ME. Structure, properties and regulation of magnesium transport proteins. *BioMetals* 2002;15:261–270. [PubMed: 12206392]
45. Kimizuka H, Koketsu K. Ion transport through cell membrane. *J Theoret Biol* 1964;6:290–305. [PubMed: 5875308]
46. Kiuchi-Saishin Y, Gotoh S, Furuse M, et al. Differential expression patterns of claudins, tight junction membrane proteins, in mouse nephron segments. *J Am Soc Nephrol* 2002;13:875–886. [PubMed: 11912246]
47. Kleta R, Bockenhauer D. Bartter syndromes and other salt-losing tubulopathies. *Nephron Physiol* 2006;104:73–80.
48. Köckerling A, Fromm M. Origin of cAMP dependent Cl⁻ secretion from both crypts and surface epithelia of rat intestine. *Am J Physiol* 1993;264:C1294–C1301. [PubMed: 8388634]
49. Konrad M, Weber S. Recent advances in molecular genetics of hereditary magnesium-losing disorders. *J Am Soc Nephrol* 2003;14:249–260. [PubMed: 12506158]
50. Konrad M, Schaller A, Seelow D, et al. Mutations in the tight-junction gene claudin 19 (CLDN19) are associated with renal magnesium wasting, renal failure, and severe ocular involvement. *Am J Hum Genet* 2006;79:949–957. [PubMed: 17033971]
51. Konrad M, Hou J, Weber S, et al. CLDN16 genotype predicts renal decline in familial hypomagnesemia with hypercalciuria and nephrocalcinosis. *J Am Soc Nephrol* 2008;19:171–181. [PubMed: 18003771]
52. Krämer BK, Bergler T, Stoelcker B, et al. Mechanisms of disease: the kidney-specific chloride channels ClCKA and ClCKB, the Barttin subunit, and their clinical relevance. *Nature Clin Prac Nephrol* 2008;4:38–46.
53. Landau D. Potassium-related inherited tubulopathies. *Cell Mol Life Sci* 2006;63:1962–1968. [PubMed: 16810456]
54. Lee NP, Tong MK, Leung PP, et al. Kidney claudin-19: localization in distal tubules and collecting ducts and dysregulation in polycystic renal disease. *FEBS Lett* 2006;580:923–931. [PubMed: 16427635]
55. Li WY, Huey CL, Yu AS. Expression of claudin-7 and -8 along the mouse nephron. *Am J Physiol Renal Physiol* 2004;286:F1063–F1071. [PubMed: 14722018]
56. Madara JL, Dharmasathaphorn K. Occluding junction structure-function relationships in a cultured epithelial monolayer. *J Cell Biol* 1985;101:2124–2133. [PubMed: 3934178]
57. Mandon B, Siga E, Roinel N, et al. Ca²⁺, Mg²⁺ and K⁺ transport in the cortical and medullary thick ascending limb of the rat nephron: influence of transepithelial voltage. *Pflügers Arch* 1993;424:558–560.
58. Martin, RB. Bioinorganic Chemistry of Magnesium. In: Sigel, H.; Sigel, A., editors. *Metal Ions in Biological Systems*. Vol. 26. New York, NY: Marcell Dekker; 1990. p. 1-13.

59. Martinez-Palomo A, Meza I, Beaty G, et al. Experimental modulation of occluding junctions in a cultured transporting epithelium. *J Cell Biol* 1980;87:736–745. [PubMed: 6780571]
60. Meij IC, van den Heuvel LP, Knoers NV. Genetic disorders of magnesium homeostasis. *BioMetals* 2002;15:297–307. [PubMed: 12206395]
61. Møllgård K, Malinowski DN, Saunders NR. Lack of correlation between tight junction morphology and permeability properties in developing choroid plexus. *Nature* 1976;264:293–294. [PubMed: 1004553]
62. Müller D, Kausalya PJ, Claverie-Martin F, et al. A novel claudin-16 mutation associated with childhood hypercalciuria abolishes binding to ZO-1 and results in lysosomal mistargeting. *Am J Hum Genet* 2003;73:293–1301.
63. Müller D, Kausalya JP, Meij IC, et al. Familial hypomagnesemia with hypercalciuria and nephrocalcinosis: blocking endocytosis restores surface expression of a novel Claudin-16 mutant that lacks the entire C-terminal cytosolic tail. *Hum Mol Genet* 2006;91:3076–3079.
64. Nightingale ER Jr. Phenomenological theory of ion solvation. Effective radii of hydrated ions. *J Phys Chem* 1959;63:1381–1387.
65. Ohta H, Adachi H, Takiguchi M, et al. Restricted localization of claudin-16 at the tight junction in the thick ascending limb of Henle's loop together with claudins 3, 4, and 10 in bovine nephrons. *J Vet Med Sci* 2006;68:453–463. [PubMed: 16757888]
66. Okada K, Ishikawa N, Fujimori K, et al. Abnormal development of nephrons in claudin-16-defective Japanese black cattle. *J Vet Med Sci* 2005;67:171–178. [PubMed: 15750313]
67. Pappenheimer JR, Renkin EM, Borrero LM. Filtration, diffusion and molecular sieving through peripheral capillary membranes. A contribution to the pore theory of capillary permeability. *Am J Physiol* 1951;167:13–46. [PubMed: 14885465]
68. Piontek J, Winkler L, Wolburg H, et al. Formation of tight junction: determinants of homophilic interaction between classic claudins. *FASEB J* 2008;22:146–158. [PubMed: 17761522]
69. Praga MJ, Vara E, Gonzalez-Parra A, et al. Familial hypomagnesemia with hypercalciuria and nephrocalcinosis. *Kidney Int* 1995;47:1419–1425. [PubMed: 7637271]
70. Rocha AS, Magaldi JB, Kokko JP. Calcium and phosphate transport in isolated segments of rabbit Henle's loop. *J Clin Invest* 1977;59:975–983. [PubMed: 856875]
71. Rodríguez-Soriano J. Bartter and related syndromes: the puzzle is almost solved. *Pediatr Nephrol* 1998;12:315–327. [PubMed: 9655365]
72. Rodríguez-Soriano J, Vallo A, Garcia-Fuentes M. Hypomagnesaemia of hereditary renal origin. *Pediatr Nephrol* 1987;1:465–472. [PubMed: 3153319]
73. Satoh J, Romero MF. Mg²⁺ transport in the kidney. *BioMetals* 2002;15:285–295. [PubMed: 12206394]
74. Schlingmann KP, Konrad M, Seyberth HW. Genetics of hereditary disorders of magnesium homeostasis. *Pediatr Nephrol* 2004;19:13–25. [PubMed: 14634861]
75. Schmitz H, Barmeyer C, Fromm M, et al. Altered tight junction structure contributes to the impaired epithelial barrier function in ulcerative colitis. *Gastroenterology* 1999;116:301–309. [PubMed: 9922310]
76. Schultz SG, Solomon AK. Determination of the effective hydrodynamic radii of small molecules by viscometry. *J Gen Physiol* 1961;44:1189–1199. [PubMed: 13748878]
77. Schulzke JD, Bentzel CJ, Schulzke I, et al. Epithelial tight junction structure in the jejunum of children with acute and treated celiac sprue. *Pediatric Res* 1998;43:435–441.
78. Simon DB, Lu Y, Choate KA, et al. Paracellin-1, a renal tight junction protein required for paracellular Mg²⁺ resorption. *Science* 1999;285:103–106. [PubMed: 10390358]
79. Stein, WD. Channels, carriers, and pumps: An introduction to membrane transport. San Diego: Academic Press; 1990.
80. Stevenson BR, Anderson JM, Goodenough DA, et al. Tight junction structure and ZO-1 content are identical in two strains of Madin-Darby canine kidney cells which differ in transepithelial resistance. *J Cell Biol* 1988;107:2401–2408. [PubMed: 3058723]
81. Suki WN, Rouse D, Ng R, et al. Calcium transport in the thick ascending limb of Henle. *J Clin Invest* 1980;66:1004–1009. [PubMed: 7430341]

82. Tang VW, Goodenough DA. Paracellular Ion Channel at the Tight Junction. *Biophys J* 2003;84:1660–1673. [PubMed: 12609869]
83. Van Itallie CM, Anderson JM. Claudins and epithelial paracellular transport. *Annu Rev Physiol* 2006;68:403–429. [PubMed: 16460278]
84. Van Itallie CM, Fanning AS, Anderson JM. Reversal of charge selectivity in cation or anion-selective epithelial lines by expression of different claudins. *Am J Physiol Renal Physiol* 2003;285:F1078–F1084. [PubMed: 13129853]
85. Van Itallie CM, Rogan S, Yu AS, et al. Two splice variants of claudin-10 in the kidney create paracellular pores with different ion selectivities. *Am J Physiol Renal Physiol* 2006;291:F1288–F1299. [PubMed: 16804102]
86. Van Itallie CM, Holmes J, Bridges A, et al. The density of small tight junction pores varies among cell types and is increased by expression of claudin-2. *J Cell Sci* 2008;121:298–305. [PubMed: 18198187]
87. Ward DT. Calcium receptor-mediated intracellular signalling. *Cell Calcium* 2004;35:217–228. [PubMed: 15200145]
88. Watson CJ, Rowland M, Warhurst G. Functional modeling of tight junctions in intestinal cell monolayers using polyethylene glycol oligomers. *Am J Physiol Cell Physiol* 2001;281:C388–C397. [PubMed: 11443038]
89. Weber S, Hoffmann K, Jeck N, et al. Familial hypomagnesaemia with hypercalciuria and nephrocalcinosis maps to chromosome 3q27 and is associated with mutations in the PCLN-1 gene. *Eur J Hum Genet* 2000;8:414–422. [PubMed: 10878661]
90. Weber S, Schneider L, Peters M, et al. Novel paracellin-1 mutations in 25 families with familial hypomagnesemia with hypercalciuria and nephrocalcinosis. *J Am Soc Nephrol* 2001;12:1872–1881. [PubMed: 11518780]
91. Weber S, Schlingmann KP, Peters M, et al. Primary gene structure and expression studies of rodent paracellin-1. *J Am Soc Nephrol* 2001;12:2664–2672. [PubMed: 11729235]
92. Wittner M, Desfleurs E, Pajaud S, et al. Calcium and magnesium: Low passive permeability and tubular secretion in the mouse medullary thick ascending limb of Henle's loop (MTAL). *J Membr Biol* 1996;153:27–35. [PubMed: 8694904]
93. Yu ASL, Enck AH, Lencer WI, et al. Claudin-8 expression in Madin-Darby canine kidney cells augments the paracellular barrier to cation permeation. *J Biol Chem* 2003;278:17350–17359. [PubMed: 12615928]
94. Zeissig S, Bürgel N, Günzel D. Changes in expression and distribution of claudin-2, -5 and -8 lead to discontinuous tight junctions and barrier dysfunction in active Crohn's disease. *Gut* 2007;56:61–72. [PubMed: 16822808]
95. Zhao L, Yaoita E, Nameta M, et al. Claudin-6 localized in tight junctions of rat podocytes. *Am J Physiol Regul Integr Comp Physiol* 2008;294:R1856–R1862. [PubMed: 18367650]

Glomerulus	Proximal tubule	Thin descending limb	Thin ascending limb	Thick ascending limb	Macula densa	Distal tubule	Collecting duct
CLDN1							
	CLDN2						
			CLDN4		CLDN3		CLDN4
	CLDN6			CLDN6		CLDN6	CLDN6
		CLDN7				CLDN7	CLDN7
		CLDN8				CLDN8	CLDN8
	CLDN9						
			CLDN10				
	CLDN11			CLDN11			CLDN14
						CLDN16?	
						CLDN19?	

Figure 1. Localization of claudin proteins in mammalian kidney. Localization data were summarized from the following studies: claudins 1, 3, 4, and 11 [46], claudin-2 [19], claudin-6 [1,95], claudins 7 and 8 [55], claudin-9 [1], claudin-10 [85], claudin-14 [7], claudin-16 [50,78,91] and claudin-19 [5,50,54]). Tubule expression of claudins 6 and 9 are only found in neonatal kidney [1]. Many of these claudins have not been rigorously examined in all nephron segments so the data shown are not comprehensive. Macula densa claudin expression is from our own unpublished results. Claudins 5 and 15 are confined to endothelial cells of the vasculature and glomeruli [46] and so are not shown. Claudins 12, 18 and 20–24 have not yet been examined. Figure modified from [4] (copyright Lippincott, Williams & Wilkins, 2007).

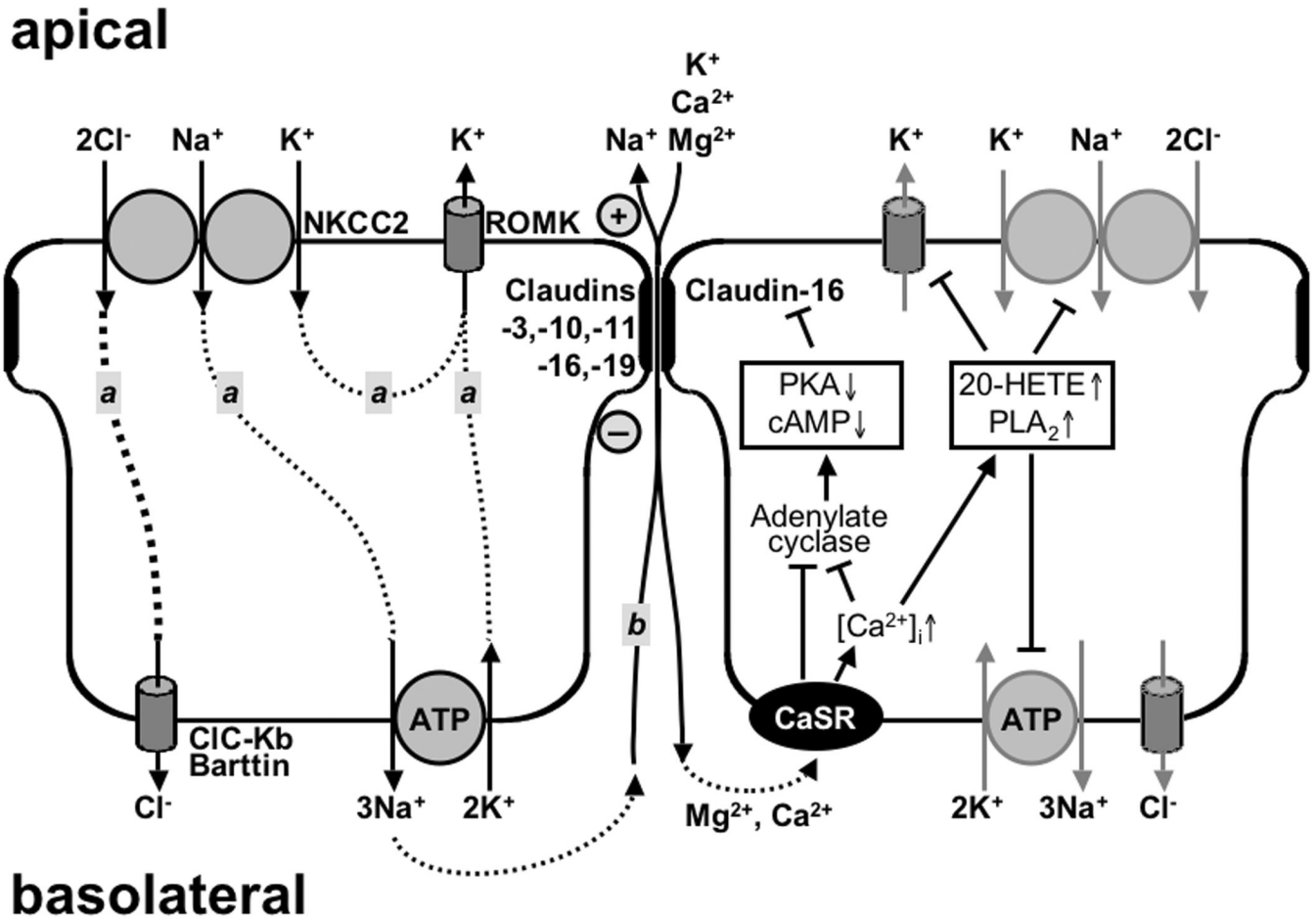


Figure 2.

Transport systems involved in the generation of the driving force for paracellular divalent cation resorption in the TAL. Left: Two components are contributing to the lumen positive, transepithelial potential. Component “a” consists of NKCC2 (Na⁺-K⁺-2Cl⁻-symport, affected in Bartter type I), ROMK (apical potassium channel, affected in Bartter type II), CIC-Kb (basolateral Cl⁻ channel, affected in Bartter type III) with its subunit barttin (affected in Bartter type IV). Component “b” is a Na⁺ diffusion potential due to a paracellular back-leak of Na⁺. Right: Mechanisms by which CaSR (Ca²⁺-sensing receptor), may modulate paracellular divalent cation transport either by affecting the transepithelial potential (inhibition of NKCC2, ROMK and Na⁺/K⁺-ATPase through a Ca²⁺ and PLA₂-dependent increase in 20-HETE) and/or through a cAMP-dependent PKA-effect on claudin-16 as proposed by Ikari et al. [41].

Table 1
Methods for the determination of paracellular permeability

Methods	advantages	disadvantages / difficulties
<i>Electrophysiological Methods</i>		
Resistance / Conductance Measurement	easy to determine	not ion-specific (always sum of cation and anion conductance) always sum of trans- and paracellular pathway
Two path impedance spectroscopy / Conductance scanning	allows discrimination between trans- and paracellular pathway	not ion-specific intricate technique
Diffusion Potential Measurement	determination of relative ion permeabilities (e.g. P_{Na}/P_{Cl}) absolute permeabilities, if combined with R^t measurements	liquid junction potentials calculation of activity coefficients limited to electrically charged solutes
<i>Flux Measurements</i>		
steady-state conditions	direct determination of absolute permeabilities, including permeabilities to uncharged solutes	requires radioactive / fluorescence labelling development or unstirred layers / transepithelial potentials
zero - trans conditions	direct determination of absolute permeabilities, including permeabilities to uncharged solutes	may affect tight junction integrity development or unstirred layers / transepithelial potentials